PUB-7 E Exp. 382

Nucl. Meth.

CLNS 419
March 1979
FERMILAB-PUB-79-137-E

A TECHNIQUE FOR LOCATING MUON DEEP INELASTIC SCATTERING EVENTS IN A NUCLEAR EMULSION TARGET

by

L. Hand, D. Petersen[a], H. Scott - Laboratory of Nuclear Studies
Cornell University, Ithaca, N.Y. 14853, U.S.A.

M. Atac, A. L. Read, L. Voyvodic - Fermi National Accelerator Laboratory,
P. O. Box 500, Batavia, IL 60510, U.S.A.

A. Dwurazny, B. Furmanska, R. Holynski, A. Jurak, S. Krzywdzinski,
G. Nowak, H. Wilczynski, W. Wolter, B. Wosiek - Institute of Nuclear
Physics, ul. Kawiory 26R, 30-055 Krakow, Poland

R. Ball, J. Kiley, A. Kotlewski, L. Litt - Physics Department
Michican State University, East Lansing, Michigan 48823, U.S.A.

J. Florian[b], J. J. Lord, R. J. Wilkes - Physics Department FM-15,
University of Washington, Seattle, Washington 98195, U.S.A.

(a) Present address: Physics Department, Indiana University, Bloomington, Indiana

(b) Present address: Laboratory of Nuclear Studies, Cornell University,
Ithaca, NY 14853, U.S.A.

INTRODUCTION

The discovery of the J/ψ particle and subsequent accumulation of evidence for the existence of charm has prompted theoretical studies which predict that charmed hadrons might have a lifetime just below the detection limit for bubble chambers, but within the range of nuclear emulsion techniques.[1] The observation of scale-breaking in deep inelastic muon scattering at Fermilab is consistent, in some theoretical models[2], with the opening of new channels due to charm production and thus motivated the construction of the apparatus described here[3] in an attempt to observe directly an example of the decay of such a short-lived particle, if these particles are relatively copiously produced in muon interactions. A system of counters, spark chambers, and magnets is used to detect and analyze the momenta of scattered muons. The emulsion target provided an intimate view of the interaction vertex, with a spatial resolution of ∿0.2 μm in individual events, using statistical fitting of silver grain coordinates.

At first sight, one would think that background from beam tracks traversing the emulsion stack would obscure any events of interest. It is empirically determined that backgrounds of up to 5×10^5 incident muons/cm^2 can be tolerated by scanners although one would prefer less than 10^5/cm^2. With a target thickness in the beam direction of 5 cm and density of 3.8 gm/cm^2, the maximum tolerable background level yields ∿5.8 events/μbarn/cm^2, which is quite a reasonable yield. With a total stack area of ∿1300 cm^2, 200 events corresponds to σ ∿1/40 μb. For muon scattering this cross section corresponds to a minimum Q^2 cutoff above 2 (GeV/c)^2 or about 0.1% of the total cross section of 20 μbarns. [In this experiment the mean value of Q^2 was about 4.6 (GeV/c)^2 and the mean value of the muon energy loss was 61.7 GeV.] It was expected that the relative yield of charmed

particles would be higher for deep inelastic scattering than for the more numerous low Q^2 events. We expect a yield (at high Q^2) of 1-2% in contrast to neutrino events which are more difficult to obtain but which are expected to yield 5-10% charmed particles. An advantage of using muons is that the charmed particles are produced in pairs.

A major difficulty in the emulsion technique is the problem of locating events in a reasonable amount of scanning time. Because the process of interest has a long mean free path, incident beam tracks cannot be followed to an interaction vertex as in experiments using hadron beams. The idea of using counter techniques to select and locate events in emulsion is not new, and several experiments using hybrid emulsion/spark chamber systems have been described in the literature.[4] However, the relatively coarse spatial resolution of conventional spark chambers ($\sim \pm 0.5$ mm) results in relatively large search volumes. Drift chambers can provide, in principle, nearly an order of magnitude increase in resolution ($\pm$ 60 μm)[5], and the system described here represents, to our knowledge, the first application of drift-chamber technology in a hybrid emulsion experiment.

Electronic Trigger and Location of Incident Beam Tracks

The layout of the electronic detector[6] is shown in Fig. 1. Since the purpose of the electronic detector in this experiment was only to identify and locate deep inelastic scattering events in the emulsion plus provide momentum analysis for the scattered muon, the basic trigger was kept very simple. An event was recorded for further analysis when it gave a coincidence of the beam defining counters, C1, C2, C3 and C4, with two of the scattered muon detectors, SA and SB. It could be vetoed by the presence of a halo particle in the HV counter, or an undeflected muon in the beam veto counters, BV_I and BV_{II}. Rejection of events

from outside the emulsion was done only in the off-line analysis to avoid any instrumental bias which might deplete the sample of good, high Q^2, events.

The location of the incoming muon was found by means of 8 proportional wire chamber planes and 6 drift chamber planes. The proportional wire planes had 2 mm wire spacing and were arranged as two sets of triplets near the target and an x-y doublet for upstream of the target. Details of their construction and operation are given elsewhere.[6] The beam drift chambers each consisted of four wires with 1/2 in. wire-to-wire spacing, (1/4 in. drift space on each side of a wire). The chambers were continuously flushed with 50% Argon-50% Ethane gas mixture,[7] chosen for its rapid saturation of drift velocity and consequent insensitivity to small variations in the electric field. The uniformity of the field across the drift space was aided by the addition of 10 field shaping wires.[8] The pulses from each wire were amplified and discriminated by electronics of FNAL design mounted on the chamber inside the aluminum chamber housing to avoid noise problems. During the run these chambers were found to have quite noise-free and reliable signals.

The discriminated signals from the sense wires were used as STOP pulses in a set of EG & G 8 channel time-to-digital-converters (EGG TD 811) with a clock frequency of 20 mHz which were given a common START by the event trigger. A single count in these digitizers corresponded to 100 psec or a displacement of about 5 μm. The number of recorded counts in a given channel was thus directly proportional to the distance, d, of the particle from that sense wire, under the assumption of a constant drift velocity V_d (discussed below).

$$d = V_d(t - t_o)$$

The parameters, then, which had to be determined for each wire (channel) were the base time, t_o, and the drift velocity. Furthermore, the alignment of the chambers with respect to each other had to be determined to within 50 μm (= .002 in.) by using fitted beam tracks, as that was beyond the accuracy of our survey. In order to get the base times for each wire, we measured the signal delay in each amplifier and discriminator and in the cable to the TDC. The time of flight between chambers was also taken into account. The counting rate was measured for each channel by generating START and STOP pulses from a pulser and varying the STOP delay by a known number of nanoseconds. When all these effects were taken into account, we should have been left with only one overall base time for all channels, which would be determined by the delay in the trigger circuitry. We quickly found in the analysis that this was not the case. We were led to the conclusion that there were significant (several nanoseconds) differences between channels in TDC's in the times it took for STOP signals to register. These times had to be fitted from the data also.

Each of the 6 chambers received its high voltage from a separate supply. There were small differences in the field in each chamber due to both the difference in supplies and the differences in loading resistors. Thus, there could be small differences between the chambers in drift velocity. However, the 4 wires within a chamber would have to be the same. We found this to be, in fact, the case with a typical value of $1/v_d$ = 188 ns/cm.

These 6 chambers were arranged with chambers 7, 9, and 11 reading out a y coordinate of the particle and 8, 10, and 12 reading x. The outside two, e.g., 7 and 11, we set with their sense wires at, very nearly, a common lateral (y) position, and the center chamber was displaced 1/4 in. with respect to them.

For the normal case of all chambers giving a clean signal, we had 6 coordinate readings in each projection for a beam track, 3 from the PWC's, and 3 from the drift chambers. The very long lever arm of the far upstream PWC's meant that our best information on the track angle came from them, in spite of the much better resolution of the drift chambers. Our drift chambers were of a pioneering design and so had no internal hardware capability of telling on which side of the sense wire the particle passed. This "left-right ambiguity" was resolved by the PWC trajectory, except in those cases where the hit was so close to a wire that both solutions were acceptable. In those events a minimum χ^2 line was fitted through all available points. The member of the ambiguous pair farthest from this line was thrown out, and a new line fitted through the surviving hits.

Several techniques were used to obtain the alignment constants and the 30 parameters needed for the beam drift chambers. The two PWC triplets were taken as the basis of the coordinate system and all other alignments found with respect to them. One of the more useful techniques was to make a "K plot" for each wire of the drift chambers*, where the displacement of the wire from a PWC particle trajectory is plotted against the time registered for that particle in the drift chamber under study. A statistical best fit over a large track sample yielded good numbers for the alignment and the drift velocity for that chamber. However, because of the poor resolution of the PWC's there was a large scatter of points on the plots and the determination of t_o for each wire was not adequate by this method. To refine these numbers we used an iterative process, where the particle's position at the center drift chamber was calculated from a line between the hits in the two outside chambers, x_c and subtracted from the hit position in

*This type of plot is called a "K plot" because the trajectory displacement is double-valued with respect to the drift time.

that wire, x_m. An incorrect t_0 will cause a bimodal distribution in a histogram of $(x_m - x_c)$. The base times were varied to minimize the width of this distribution. Such an approach is possible, of course, only because of the staggering of the chamber wires. Even so the problem is not mathematically completely determined, and the technique is useful only for refinement of base times that are known approximately.

A study of the characteristics of the bimodal distributions indicated that the individual drift chambers should have been capable of resolutions of about 80-100 μm. However, largely because of the unanticipated difficulties with the parameters of the chambers, we only achieved an overall resolution* (σ) for the system of about 200 microns. In the process of studying the resolution of the chambers, we investigated possible non-linear effects in the drift time. In particular, we took the hypothesis of a constant mean free path and developed a simple, first order, formula for non-constant drift velocity. We found that such effects were completely unobservable in our data.

The method used to link the chamber coordinate system to the emulsion coordinate system is discussed in detail below.

EVENT IDENTIFICATION

The 150 GeV muon beam was parallel to better than ±2 mrad. with a hadron contamination $\leq 2 \times 10^{-5}$. A spectrometer using magnetized iron toroids[6] provided identification and momentum analysis of the scattered muon with a precision (sigma) in 1/p of ∿±15%.

>99 percent of the triggers in this experiment resulted from interactions in the 2 meter iron muon shield (see Fig. 1). The problem for the electronic analysis was to identify the <1% which occurred in the emulsion, to tell the

*This resolution was determined empirically by the internal consistency of straight line fits to beam tracks.

emulsion scanners where to find them, and give the scanners enough identifying characteristics so that when they located an event, they could tell it from one of the plentiful background of very low Q^2 events and hadronic events. (Typically, 4-5 low Q^2 events were found in the scan volume for a high Q^2 event).

The first step was to reconstruct the tracks in the four sets of spark chamber planes immediately downstream of the muon shield. Each set of planes consisted of x, y, u and v planes (u and v at 45° to x and y) and was thus capable of distinguishing 3 dimensional tracks. The track finding procedure was to search for the best track in these sets of chambers (a maximum of 16 sparks), remove all sparks on that track from the sample, and reinitiate the search. The fitting continued until the minimum criterion of 7 sparks per track could no longer be satisfied.

Because of the long memory time of the spark chambers, they could hold halo tracks; we therefore could not expect that the spectrometer register only scattered muon tracks. Each track found had to be tested to see whether it was a muon from the emulsion target. Our definition of an event muon was that it project back to within 4.0 cm of the beam track at the target center and have a deflection greater than 6.5 mrad. This made a generous allowance for multiple scattering in the iron and passed a few events originating in the shield.

The second step was to reconstruct all possible tracks in the downstream proportional chamber-drift chamber system. The 6 downstream drift chambers were each 24-wire planes with 2 cm wire spacing. Their signals were read by a LeCroy 2770 multi-time digitizer, for which each wire signal was a START and the event trigger was a STOP. This avoided the problems of having to delay a large number of signals for a long time, but made these susceptible to noise problems from after-pulses. This was solved by mounting single shot discriminators on the

chambers. The operating parameters for these chambers were found by similar methods to those for the upstream chambers using beam tracks.

However, two fundamental limitations of drift chambers became significant in this application, because of the high multiplicities of events. If two or more particles traversed the same cell, only the one closer to the wire would be recorded. Also, occasionally a particle would produce a δ-ray which headed toward the sense wire and gave a false reading. The track fitting had to contend therefore with both missing points and false points.

A track in the downstream system was defined as having at least 3 of the 5 possible points, in any one view. It was not usually possible to correlate tracks between views. Two point tracks were allowed only where the angle was so large as to preclude finding more than 2 points. All tracks had to project to within 10 mm of the incident track at the center of the target. Even so, it was not possible to completely eliminate false tracks and so points were not eliminated from the sample for further track fitting as they were for the spark chambers. In particular, the left-right ambiguity of the sense wires usually caused wide angle tracks with only 2 hits and, therefore, 4 hit images to produce more than one line which satisfied the selection criteria. When a complete set of possible tracks was obtained, shared hits*, if any, were deleted from the track with the worse χ^2 and the affected track refitted. Our initial hope in this process was to produce reliable z coordinates+ for the vertices. However, it soon became evident that the probability was so high for the production of secondary vertices in the target that our z calculation could not be counted on and a different procedure was devised.

---

*i.e., hits contributing to more than one track.

+The z coordinate is the beam direction.

We could then generate a preliminary scan list of likely events. An event was selected for inclusion in the list if:

1. it had a good beam track

and

2. it had an acceptable scattered muon in the spectrometer

or

it had 2 or more tracks reconstructed in at least one view of the downstream PC-DC system.

This cut our initial sample of about 10^5 triggers to about 1200. Each of these selected events was then looked at with a program which would display a reconstruction of the event on a Tectronix 4010 graphics terminal. One selected the x or y view and the program drew the emulsion, each chamber with the hits in that chamber. The muon track reconstructed from spark chamber data, and all tracks found in the proportional chamber-drift chamber system. The program for the event vertex could also enlarge any section of the event. This allowed a close look at reconstructed lines in the target region and a scanner decision on a z position. Every event in the sample was scrutinized by a physicist who evaluated its potential interest.

This process quickly revealed that the large number of events were caused by 1) the passage of a halo particle which escaped the veto, 2) an event in the downstream iron absorber which gave a track which happened to point to the emulsion, or 3) a $Q^2 \approx 0$ event in the emulsion which had one, essentially undeflected muon track and one very wide angle track. This cut the number of events to be searched for to 269. A list of these remaining events with their coordinates and copies of their computer reconstructions were forwarded to the emulsion scanners. Also, a horizontal projection of the event was generated with all of the tracks drawn at their actual angles as they would seem through the

microscope, for direct visual comparison. Such event pictures are shown in Figures 2-3. Figure 4 and 5 contain statistical information about the comparison of drift chamber information with emulsion tracks for tagged events.

EMULSION AND CHAMBER COORDINATE SYSTEMS

Great care was taken in the preparation of this experiment to provide sufficient references for each emulsion stack to locate its coordinate system accurately with respect to the outside world. Ilford K5 emulsion was purchased in pre-cut pellicles measuring (nominally) 7.5 x 5.0 x 0.06 cm. Stacks were assembled from 85-100 pellicles to produce a solid block of emulsion 7.5 x 5.0 x ∿7.0 cm. [The stacks were placed in the beam with the pellicles horizontal and the beam parallel to the 5 cm dimension]. Twenty-six stacks were prepared, for a total of about 6.5 litres of emulsion. Two of the stacks were made from an older batch of Ilford G5 pellicles. Background exposure before the experimental run totalled approximately 6 months at sea level and about 12 hours at jet altitude.

Each of the stacks was then clamped by two aluminum bars fastened with four 3/8" diameter stainless steel threaded rods. Lucite spacers kept the emulsion from contacting aluminum, with which it would react chemically. The aluminum bars were machined to close tolerances, and the lower bars were selected to be identical to within ±0.001" (25 μm) in all dimensions. The front and left side faces of the emulsion stacks were next milled flat and parallel to the corresponding faces of the lower aluminum clamp bar. The machinist measured and recorded the locations of four points on each machined face with respect to the aluminum reference surfaces, as well as the vertical thickness of the stack at each corner. Finally, a scribe mark was made across the front face of the emulsion at an angle of 50° above horizontal. This scribe line was crucial to finding the vertical position of a pellicle, since pellicle thickness varied by up

to 20%. Figure 6 shows a completed target assembly.

During exposure, the stacks were mounted on an aluminum stand bearing three locating pins to contact the lower clamp bar of each stack. Tests showed that the stacks could be removed and replaced with an error of less than 0.002" (50 μm). Each stack was used until a track density of 3-5 x 10^5 muons/cm^2 was accumulated. Immediately following exposure, the stack measurements made after emulsion machining were repeated, to detect possible changes caused by emulsion responding to environmental factors. Differences were negligible in most cases. The stacks were then unclamped and sent to Seattle for processing. Due to the high ($\geq$200 lb/in^2) clamping pressure used, the pellicles tended to stick together in a solid block, even after the clamping members were removed.

Each of the pellicles was contact-printed with a reference grid prior to development. The grid printing apparatus consisted of a lucite top plate equipped with guide bars and a grid negative*, and a small lamp approximately 1 m from the printing surface, whose intensity and duration were controlled by an autotransformer and timer switch. The machined surfaces of an emulsion stack were pressed agsinst the guide bars, the bottom pellicle was gridded, peeled off the stack and mounted, and the process repeated. Each pellicle was numbered with a sharp pencil, which left pressure marks that would come out in development. Thus, each pellicle's grid was applied before any mechanical distortions could be introduced by the rather rough peeling and mounting procedure.

Pellicles were mounted on specially-treated glass obtained from Ilford. They were developed by the two-temperature method[9] and had typical grain densities for minimum ionizing tracks of ∿19-20/100 μm.

---

*Kindly supplied by Prof. H. Heckman of LBL.

The actual location of the emulsion stacks with respect to the electronics coordinate system was determined by preparing a small emulsion stack of 10 pellicles and exposing it to a very low density of incident muons. The trigger requirements were altered so that every incoming muon was recorded. Their trajectories were reconstructed and their coordinates at the front face of the emulsion were computed and plotted. The entire volume of the low density stack was scanned for beam tracks, and the location of each at the front face was plotted. An overlay of the two plots yielded the relation of the two coordinate systems. This left only small stack-to-stack variations caused by the mounting procedure in changing emulsion targets.

EVENT SEARCHING IN THE EMULSION

The stacks were equally divided between the two emulsion groups (Krakow and Seattle) for scanning. Since the upstream drift chambers provided an accurate estimate of the location at which the beam track initiating an interaction entered the front face of the emulsion stack, and the vertexing information provided by the downstream chambers gave a less accurate estimate of the event location, it was decided to use the beam track coordinates to define the transverse location of the event, and the downstream data to indicate the approximate event vertex location along the beam direction. Due to the shallow production angles characteristic of high energy interactions, as well as the secondary vertices mentioned above, the vertexing problem was inherently ill-conditioned, and in many cases it was necessary to scan the entire length (5 cm) of the plate; however, with sufficient transverse accuracy, the scanning volume was still manageably small. The average scanning volume was 250 mm^3/event and about 190 mm^3/found event. The total volume searched was about 68 cm^3.

In transforming a drift chamber prediction of event location into a scanning region, stack-to-stack and plate-to-plate corrections were found to be necessary. As noted, each pellicle was contact-printed with a grid of numbered 1 mm x 1 mm squares. Distortions in the grid negative were measured and parametrized, so that one could compute the true distances of each grid line from the grid edge. The grid edge did not necessarily coincide with the pellicle edge, due to placement error during grid printing, but these offsets could be determined by measuring the actual distance from the edge to the first grid line. Thus, positions relative to grid lines could be converted into absolute distances from machined pellicle edges. The distance between the scribe mark notch (which was clearly visible on the front edge of the processed plates) at the emulsion-glass interface and the machined side edge was measured on each pellicle; this gave the height of the bottom surface of the pellicle. All measurements described were made on the lower surface of the emulsion, where dimensions are least affected by distortions due to processing shrinkage. Measurements were made on a measuring stage, with least-count of 1 μm.[10]

The scanning procedure was:

1) Given the x and y coordinates of an event from beam track drift and proportional chamber data and assuming a constant (average) pellicle thickness, an initial estimate was made of the plate number and y-square (grid coordinate) location of the muon's entry point at the front face of the stack.

2) The scanner determined the notch location (hence actual x coordinate) of the specified plate, and if necessary, moved up or down a plate or two.

3) Having determined the correct plate, the scanner measured the grid offset of the plate, and corrected the y-square estimate.

4) The scanner locates the point at which the muon entered the front edge of the plate, and began scanning across the pellicle. Although the pellicles were not in general perfectly parallel to the beam direction, this caused no difficulty, since the scanner simply followed the trend of nearby beam tracks in moving across the plates; all locating was done in a single plane (the front face), and beam tracks provided a convenient reference to compensate for tilts and distortion. Although the locating procedure seems complex, a system of scanning forms and visual aids made the calculation and locating procedure routine.

Scanning was performed using standard binocular microscopes equipped with 10x air objectives and 15x wide-field oculars. Higher powered oil lenses were used to examine objects of interest encountered during scanning. The arrangement described provided sufficient magnification (225x) to obtain high efficiency for finding events with 3 or more black, i.e., heavily ionizing, tracks while keeping worst-case scanning time around 6 hours/event. The typical scan time was about 2 hours/event. Twenty-six events not found by this procedure were searched for later at higher magnification (450x) and five tagged events were found in this way.

Initially, a path 1-2 mm wide was scanned across each of 3 to 5 plates. As events were found and identified, their deviations from the predicted location were measured by tracing the beam track back to the front edge of the plate and inverting the location procedure. Stack-by-stack variations in the average offset were found, probably as a result of inadequate mechanical clamping in the stack changing process, so a running average offset was tabulated for each stack, updated each time a new event was found, and this offset was included as a final correction factor in the locating procedure. Thus, each event found in a given stack helped improve the locating accuracy for subsequent events, and the search

volume could eventually be reduced to a total width of 1 mm (approximately one field of view at 10x15 magnification). Figure 7 shows the distribution of deviations $DY = Y_{found} - Y_{predicted}$ and DX for 98 events after removal of stack offsets. The DY distribution is well represented by a gaussian distribution plus a non-gaussian tail with $\sigma = 0.23$ mm. This means that the uncertainty in locating an event is dominated by the electronic uncertainty from the beam drift chambers, which was of comparable magnitude.

When an interaction was found, it was necessary to identify it positively as the sought-for event. The scattering angle θ_μ of the muon is known, and can be checked against the production angles of secondary tracks measured in emulsion. An event was considered tagged if a minimum-ionizing track was found within 10 mrad of the muon direction in space as determined by the spark chamber data. The 10 mrad cutoff was fixed by studying the distribution of $\Delta\theta$ (angle between predicted direction of scattered muon and the closest track observed in the emulsion) for a sample of 98 event candidates. The primary cause of $\Delta\theta \neq 0$ is multiple scattering in the "muon identifier." Three of these events are lost when the cuts $\Delta\theta < 10$ mrad and $\theta_\mu > 8$ mrad are made. In addition, in a subset of the data, drawings made of track patterns from emulsion measurements were compared to the drawings made from drift and proportional chamber data, and clear correlations were obtained for 53 events with $\Delta\theta < 10$ mrad, while the events with larger $\Delta\theta$ showed poor correlations. Figure 8 shows an angular distribution for tagged and untagged events for the track closest to the scattered muon direction.

Most of the four or five events typically found in the search volume were low Q^2 events and thus contained a $\theta_\mu \sim 0^\circ$ muon.

The chance of including an untagged event in the data sample if we make the cuts $\theta_\mu > 8$ mrad, $\Delta\theta < 10$ mrad is estimated from the data to be 15 percent The chance of rejecting a real event by this procedure is estimated to be about 5 percent. The tagged events are thus contaminated by an estimated background of 15% of untagged events. This could be reduced significantly if the ~ 3 mrad uncertainty in the muon angle resulting from measurement error and multiple scattering could be reduced at least a factor of 2 or if better use could be made of the downstream drift chamber information.

Figure 9 shows a scatter plot of $\Delta\theta_x$ and $\Delta\theta_y$ both for real tagged events and for background events found in the search volume. The width of the $\Delta\theta$ distribution for tagged events is clearly much narrower than the cut of 10 mrad.

The overall efficiency to find an event was 38%. The loss of real events when scanning is due partly to the failure to see events with a small number of black tracks (N_H either 0 or 1). If this were the only source of event loss, the efficiency would be about 70%.[11] The number of events in the search sample (269) agrees well with the prediction of 260 events ($Q^2 > 1$, $E'_\mu > 15$ GeV) based on a calculation in which the apparatus acceptance and finite beam size is taken into account. However, it is possible that this agreement is fortuitous, since the calculation is a sensitive function of the scattered muon angular cutoff at the minimum scattering angle.

A number of the events in the search sample ($\sim$10%) did not have a reasonable value of the momentum from the fit to the secondary muon track. Either the fitted momentum was too high or a good chisquared was not obtained for any value of the momentum. It was not possible to discover the source of this problem, but if these are assumed not to be real events, the calculated tagging efficiency would be correspondingly increased. In the most extreme case if the sample of good

events were reduced to 230, about 160 would have $N_H \geq 3$, so the efficiency (for $N_H \geq 3$) would be 98/160 = ∿65% after correction for scanner losses due to low N_H.

A rescan under low magnification was done on the majority of the events searched to determine the scanner efficiency for $N_H \geq 3$. This is believed better than 95%. Possible reasons for the remaining 35% loss are: a) overly restrictive electronic or analysis selection criteria, b) four stacks had very low efficiency. An additional tungsten target was present in these runs and may have reduced the efficiency for unknown reasons.

SEARCH FOR SHORT LIVED DECAYS

Our original intention was to search for both charged and neutral short-lived decays in the region near the tagged events. Scanners were instructed to follow all grey and minimum ionizing tracks for a distance of up to 3 mm. Any kinks observed were noted. It was not usually possible to follow the tracks for the full distance because the track either left the downstream target edge or passed into the plate immediately above or below the one containing the vertex. Ninety-five events were scanned in this way. On the average, 2.5 grey and 7.6 relativistic ($\langle n_s \rangle$-1) tracks/event were followed. The total minimum ionizing track length was 160.6 cm. Two secondary interactions were found (about 4 would be expected). These were of the type 1 + 1 and 8 + 2 ($N_h + n_s$) in events 139-2760 and 155-280 respectively. The criterion for recording the existence of a kink was an apparent angular change of $>0.5^o$. Eight kinks were located in this way. Subsequent track measurements, using standard multiple scattering techniques and measurements of adjacent tracks to check for distortions, revealed that only 3 of these kinks were inconsistent with distortions or multiple scattering, one being a 8°-9° kink in a grey track in event 156-250, a second kink of 4° in event 117-31, and still

another being a 7^0 kink in a track later found to be a 40 MeV/c electron (event 153-2237). In the first two of these events there was nothing visible which could be interpreted as the production of a pair of short-lived particles. The analysis of these events will be reported elsewhere. One K decay (K identified by multiple scattering and ionization) was observed.

The search for neutral decays was much more difficult due to the background from muon beam tracks. Only a subset of the data was searched for neutral vees. Two different search volumes were used: a) a 90^0 cone with the vertex at the apex and extending 300 microns downstream of the event; b) a rectangular parallelpiped of length 1000 microns and width 80 microns, with the long axis centered along the projection of the beam track through the vertex. Scan a) was done on 53 events (26 events out of the 53 also searched under b)). No neutral vees were seen, although 3 electron pairs from gamma conversion were located in a) and 7 pairs in b). It is very difficult a priori to calculate our efficiency for seeing neutral charmed particle decays and it is unlikely that these decays would have been seen even if they were present at the 1-2% level.

CONCLUSIONS

Theoretical estimates of charm production predict that about 1%-2% of the events in this Q^2 range should be charmed particle pair production. This means that we would have expected, on the average, one event in the data sample. A possible candidate for such an event is being studied further at this time.

Tagged deep inelastic muon events have been observed successfully in an emulsion target. Ninety-eight events out of an electronically identified sample of 269 events were found in the emulsion and a search for short-lived decays of charged particles was carried out. Partly understood losses of events reduced our data sample to a level where only one event involving charmed

pair production could have been expected making the result of this experiment inconclusive. The viability of the basic technique has been demonstrated and awaits a future experiment which will obtain more events. The techniques for searching for charmed particle decays once an event has been located need to be greater improved and speeded up. Better track efficiency in the downstream detectors would have allowed a quantitative comparison between the number of tracks seen there and at the interaction vertex, thus generating a smaller subset of the data to be searched for charm.

Provided that automatic or semi-automatic techniques for handling events can be developed, the experiment can also be improved by reducing the minimum Q^2 so that more events are obtained. Although, if theoretical predictions are correct, this should have the undesirable effect of decreasing the yield of charmed pairs from 1% ($Q^2 > 5$ GeV/c^2) to 1/3% (all Q^2), a factor of 100 could have been gained in the <u>same exposure</u> if $Q^2 = 0$ scattered muons could have been recorded. This would have given us 25,000 tagged events with 100 charmed pairs.

The use of drift chambers was a partial success. In the upstream position, as beam chambers they played an essential role. Downstream information, however, was of little use as the track reconstruction efficiency was very low. Some z information could be derived from this, but no judgement was possible about extra tracks, etc. The reason for this remains unclear, but it may be due to secondary interactions and electromagnetic showers in the emulsion target. A particular problem was caused by the very large number of extra hits, which did not seem to be track-associated. These may be due to soft photons from the event or delta-rays.

ACKNOWLEDGEMENTS

We would like to thank a number of people for both assistance and encouragement during the construction, running and analysis phases of this experiment. In particular, we thank L. Mo and S. Herb for help with the apparatus, A. Skuja for an outstanding job of tuning the muon beam. E. Friedlander contributed to the event analysis. We would also like to acknowledge the help of the staff of the Fermi National Accelerator Laboratory, especially R. Orr and E. L. Goldwasser. Finally, we thank the scanning staffs in Krakow and Seattle for their patient and skillful work.

This work was supported by the National Science Foundation and the Department of Energy, and this support is gratefully acknowledged.

REFERENCES

1. Theoretical studies on charmed particle lifetimes include:

   M. K. Gaillard, B. W. Lee, J. Rosner, Rev. Mod. Phys. 47, 277 (1975)

   J. Ellis, M. K. Gaillard, D. V. Nanopoulous, Nucl. Phys. B100, 313 (1975).

   A. J. Buras, Nucl. Phys. B109, 373 (1976).

   An experiment which may have observed the decay of a charmed baryon (produced by a neutrino) is: E. H. S. Burhop et al., Phys. Lett. 65B, 299 (1976).

   A second event has been seen in a CERN experiment: C. Angelini et al., Univ. of Brussels, preprint 1979.

2. H. T. Nieh, T. T. Wu, C. N. Yang, Phys. Rev. Lett. 34, 49 (1975).

   This paper refers to ψ/J production by muons. More recently, many authors have tried to calculate charm production by muons. An incomplete list includes:

   H. D. Politzer, Harvard Preprint HUTP-77/A038.

   V. Norikov, M. A. Shifman, A. Z. Vainshtein, V. I. Zakharov, Moscow Preprint ITEP-12.

   F. Halzen, D. M. Scott, Wisconsin preprint COO-881-8, Oct. 1977.

   M. Gluck, E. Reya, "Deep Inelastic Quantum Chromodynamic Charm Leptoproduction", DESY Preprint 79/05, Jan. 1979.

   See also the discussion of a simple vector-dominance estimate in the Fermilab proposal for E382 (unpublished).

   A simple argument suffices to make the estimate used in this paper. If we assume charmed particle photoproduction to be $\sim$10 times the measured ψ/J photoproduction, we estimate $\sigma_{charm} \sim 0.3$ μbarn at $Q^2 = 0$. For $Q^2 > 0$ the dominant part of the cross section goes as $(Q^2 + m_\rho^2)^{-1}$ while the diffractive production of charmed particles is expected to go like $(Q^2 + m_{\psi/J}^2)^{-1}$ and hence be enhanced relative to the uncharmed part at high Q^2.

   This type of estimate gives a large fraction of the observed scaling violation in muon scattering (see Ref. 6). The conventional viewpoint is that the observed scaling violation is due to QCD. The above references try (with

differing conclusions) to reconcile these. Most theorists now believe that the dominant effect is due to QCD rather than charm production, but experimental proof is lacking.

3. Experiment 382 at Fermilab. Published works on the non-charmed aspects of this experiment are: "Hadron Production in Deep Inelastic Scattering of 150 GeV Muons in Nuclear Emulsion", L. Hand et al., Acta Physica Polonica B9, 11, 1087 (1978) and "Intranuclear Cascading in Deep Inelastic Scattering of 150 GeV Muons in Emulsion", L. Hand et al, Krakow Internal Report INP-1019/PH (1978), submitted to Zeitschrift fur Physik.

4. E. H. S. Burhop et al., ref. 1 above.
   Duff, et al., Nucl. Instr. & Methods 29, 351 (1964).
   Dauber et al., Nucl. Instr. & Methods 84, 199 (1970).
   Goza et al., Rev. Sci. Instr. 41, 219 (1970).

5. Filatova et al., Nucl. Instr. & Methods 143, 17 (1977).
   The figure of 60 microns resolution refers to ideal test beam conditions.

6. Y. Watanabe, Cornell thesis 1975; see also, Y. Watanabe et al., Phys. Rev. Lett. 35, 898 (1975) and C. Chang et al., Phys. Rev. Lett. 35, 901 (1975). For a more recent discussion of the experimental evidence for a scaling violation see the summary talk by L. Hand, Proceedings of the 1977 International Symposium on Lepton and Photon Interactions at High Energies, Hamburg (1977).

7. M. Atac and J. Urish, 1978 Vienna Wire Chamber Conf. Proc. (to be published in Nucl. Instr. & Methods).

8. M. Atac, W. E. Taylor, Nucl. Instr. & Methods 120, 147 (1974).

9. A variant of the Bristol formula given by Prof. W. Barkas in his book "Nuclear Research Emulsions, V. I" (Academic Press, N.Y., 1963) was used.

10. At Seattle, a Koristka R4 microscope and a measuring stage constructed at LBL was used (Hodges, J. "Equipment for Nuclear Emulsion Analysis", UCRL 9089, U.C.-LBL 1960).

At Krakow a KSM-I microscope and MBI-9 microscope made in the USSR were used to measure event location and track angles.

11. The black tracks observed are presumed to be nuclear evaporation protons. These appear to show a universal distribution for all high energy interactions. The distribution in N_H agrees well with fits to hadron data for $N_H \geq 3$, but there is significant loss for lower N_H. The N_H distribution for $N_H \geq 3$ fits the function exp. $(-.12\ N_H)$.

FIGURE CAPTIONS

1. Experimental arrangement of FNAL experiment 382. PC1-PC12 - proportional chambers, DC1-DC12 - drift chambers, SC1-SC9 - spark chambers, C1-C5 - beam counters, HV - halo veto counter, BV1, BV2 - beam veto counters, MI1-MI4 - muon identifier counters, M1-M8 - spectrometer magnets. The trigger used was $C \cdot S \cdot \overline{BV} \cdot \overline{HV}$, where $C = C1 \cdot C2 \cdot C3 \cdot C4 \cdot C5$, $S = SA \cdot SB \cdot SC$, $BV = BV1 \cdot BV2$.

2. a) Downstream drift and proportional chamber reconstruction of an event 156-1204, vertical projection plane. Beam moves from left to right. The first object encountered is the emulsion stack (EM) with 1 cm grid lines superimposed. Next are pictured 3 drift chambers (DC) and 2 proportional chambers (PC). Data points in these chambers are noted by x's and the drift chambers have 2 x's for each data point to account for the inherent left-right ambiguity (in fact, data points look rather like thick dashes instead of x's -- this is because the picture is a hard copy from a graphics terminal). Five tracks fitted to the data points are drawn as full lines. Scattered muon track reconstructed from muon spectrometer is indicated by a dashed line. In fact, it coincides nicely with one of the tracks found in the PC-DC system.

   b) The same event reconstructed from measurements in emulsion. The expected data points are indicated by x's. Full lines represent hadron secondaries, whereas scattered muon is pictured by a dashed line. Track directions agree within $\pm 1^{\circ}$ with those reconstructed in the PC-DC system.

3. Enlarged vertex section of an event 156-1204. Fig. 3a - vertical projection plane, Fig. 3b - horizontal projection plane. Such pictures were used to estimate the location of the vertex along the muon beam. The position where an event was actually found in emulsion is indicated by an arrow (Z_{EM}). Dotted and dashed lines indicate incident and scattered muons respectively.

4. Number of one-projection tracks N_{PCDC} reconstructed in the downstream PC-DC system versus the number of tracks N_{EM} emerging from the corresponding primary interaction in emulsion. Only tracks which either were constructed out of at least 3 points or should yield 3 or more points in the PC-DC system are taken into account. Both X and Y projections contribute to the scatter plot so that each event enters twice. Positive correlation is clearly seen, especially for events originated in the downstream half of emulsion stacks ($2.5 < Z < 5.0$ cm, lower plot) where secondary interactions and gamma conversions in emulsion target contribute less additional tracks than in the upstream half ($0. < Z < 2.5$ c upper plot). This effect is also seen when one compares the average number of tracks found in the PC-DC system for these two subsamples.

5. Number M_{PCDC} of those one-projection PC-DC tracks whose directions agree to within $\pm 1.5^{o}$ with emulsion tracks versus the number N_{EM} of all tracks seen in emulsion. As before only 3 or more point tracks are taken into account and both projections contribute to the two plots. In about 50% of events, all tracks match in at least one projection.

6. Emulsion stack assembly. Twenty six of these stacks were used in the experiment.

7. Accuracy of vertex location in the direction perpendicular to the muon beam (Fig. 7a - upper histogram) and along the muon beam (Fig. 7b - lower histogram). In Fig. 7a deviations in both X and Y directions are combined, so that each event enters twice to the histogram. The stack offsets are removed. Apart

from tails ($|\Delta X,Y| > 0.6$ mm) the distribution can be represented by a gaussian distribution with $\sigma = 0.23$ mm. In Fig. 7b Z_{pred} is an average between the two (X and y) projection estimates from the drift chamber data. The influence of secondary interactions and cascading is clearly seen -- events found in the upstream half of emulsion stacks ($0.0 < Z_{EM} < 2.5$ cm, non-shaded area) have large positive displacement of about 1.4 cm, whereas events originated in the downstream half of the stacks ($2.5 < Z_{EM} < 5.0$ cm, shaded area) have net displacement of about -0.4 cm.

8. Space angle deviations between the direction of scattered muon (determined from the muon spectrometer) and the closest track observed in emulsion. The cut for the track closest to the scattered muon was $\theta_\mu > 8$ mr. Full line histogram depicts tagged muon events. The background is described by a dashed line. To estimate the background, fake muon angle predictions were assigned to each event search volume. The number of false event combinations was 268 * 147 (269 - 1 fake predictions and 147 search volumes with full information on angular distribution for all interactions found). Background was constructed by taking into account only untagged events. Thus, the chance of including an untagged event in the high Q^2 data sample, if one makes cuts $\theta_\mu > 8$ mr, $\Delta\theta_\mu < 5$ mr, is estimated to be 7%; for cuts $\theta_\mu > 8$ mr, $\Delta\theta_\mu < 10$ mr the background amounts to 15%.

9. Scatter plot of $\Delta\theta_x$, $\Delta\theta_y$ for tagged events (solid circles) and background (untagged) events (crosses) selected with $\theta_\mu > 5$ mrad.

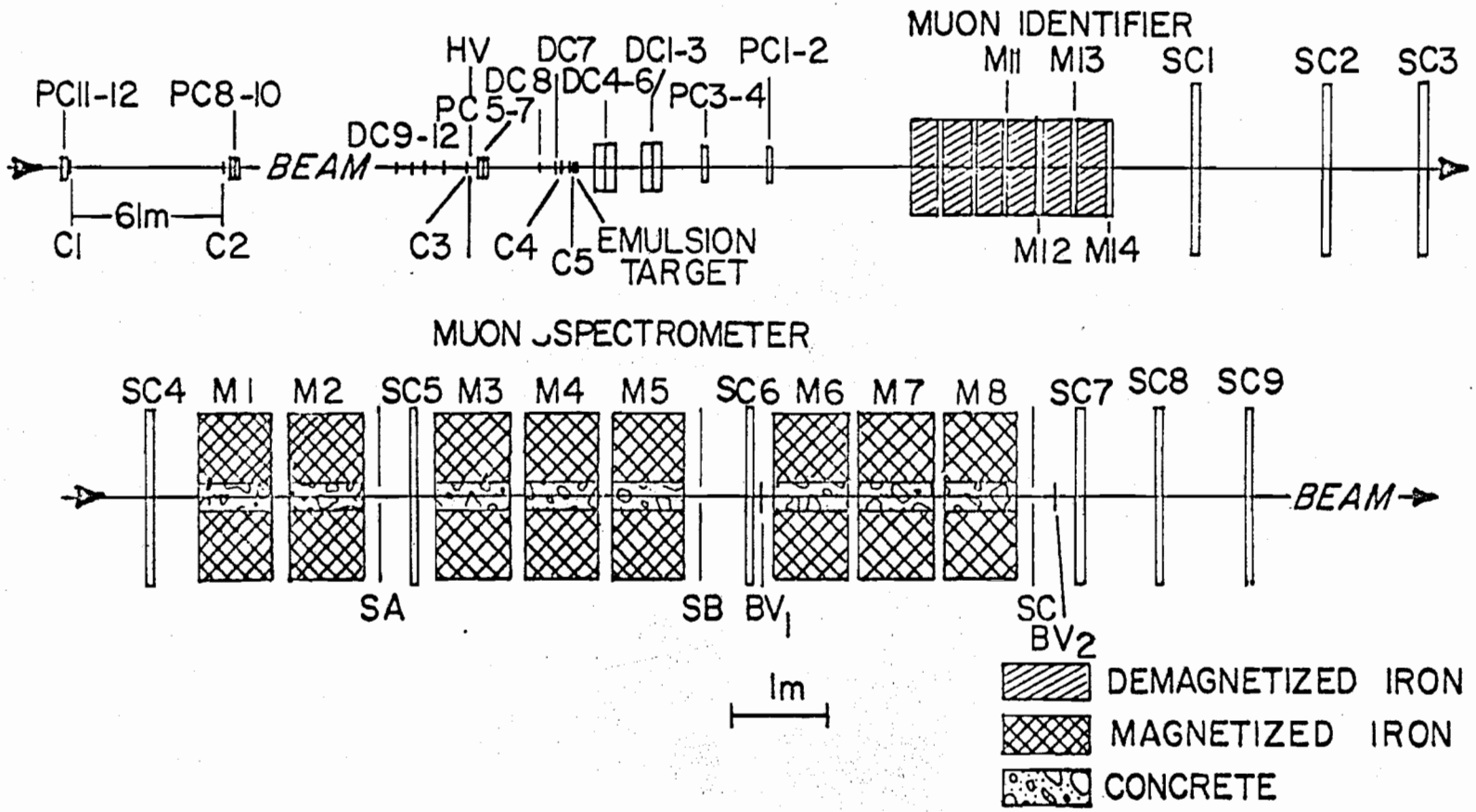
MUON IDENTIFIER
PC11-12
PC8-10
HV
DC7
DC1-3
PC1-2
DC8
DC4-6
PC5-7
PC3-4
DC9-12
BEAM
6lm
C1
C2
C3
C4
C5
EMULSION TARGET
M11
M13
SC1
SC2
SC3
M12
M14
MUON SPECTROMETER
SC4
M1
M2
SC5
M3
M4
M5
SC6
M6
M7
M8
SC7
SC8
SC9
BEAM
SA
SB
BV1
SC
BV2
1m
DEMAGNETIZED IRON
MAGNETIZED IRON
CONCRETE

Figure 1

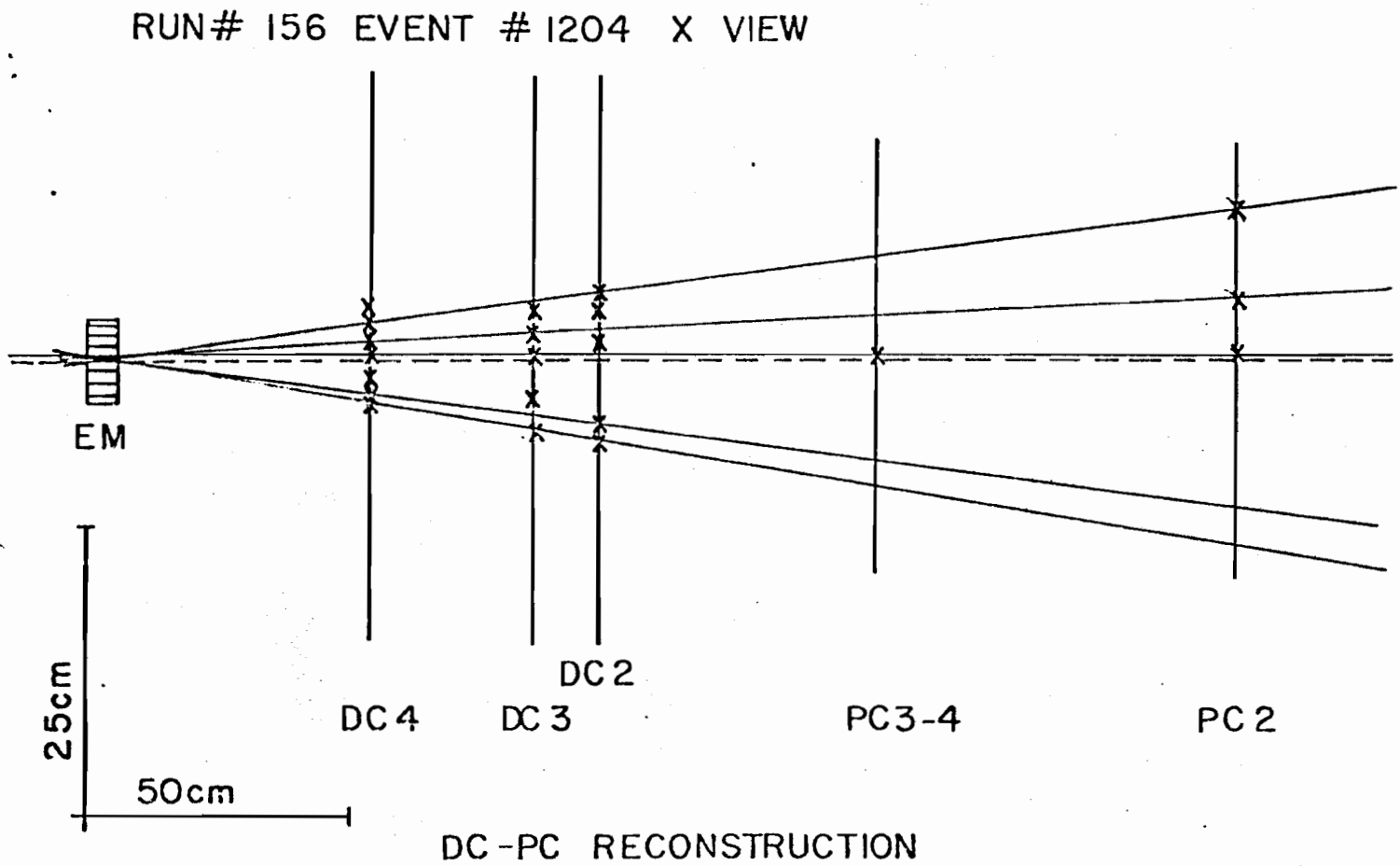

Figure 2a

0230279

RUN 156 EVENT 120401 X VIEW

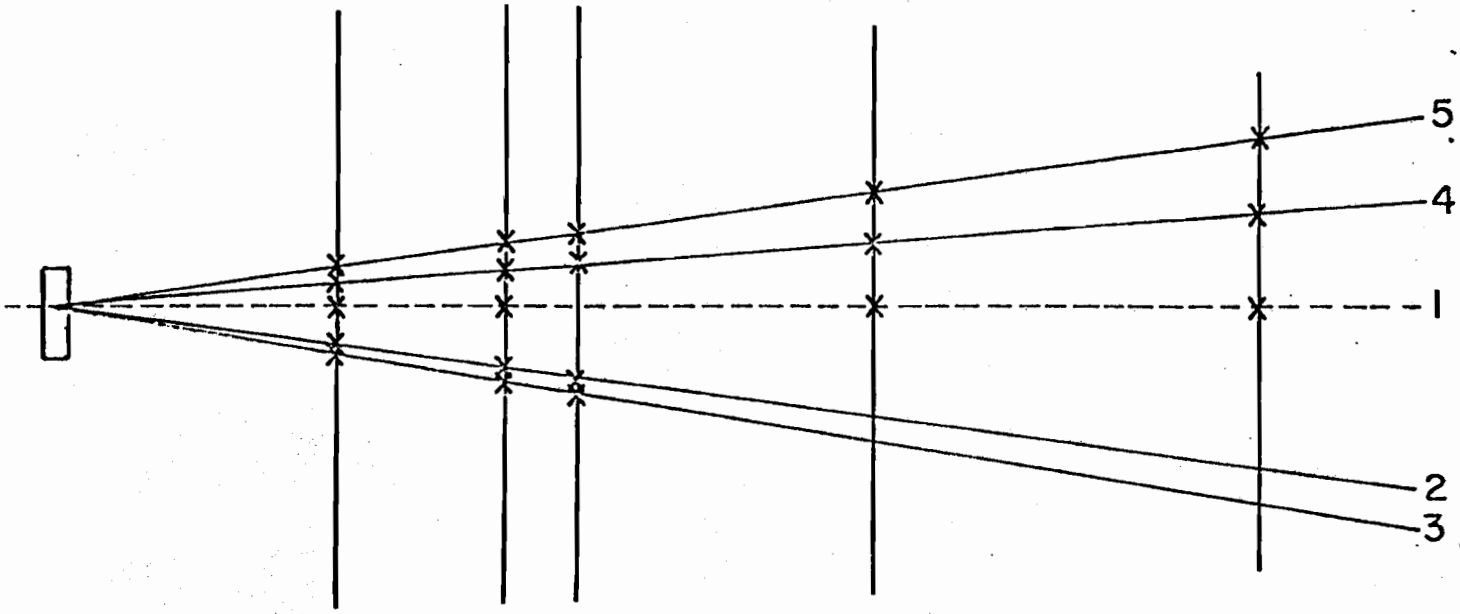

EMULSION RECONSTRUCTION

Figure 2b

029C279

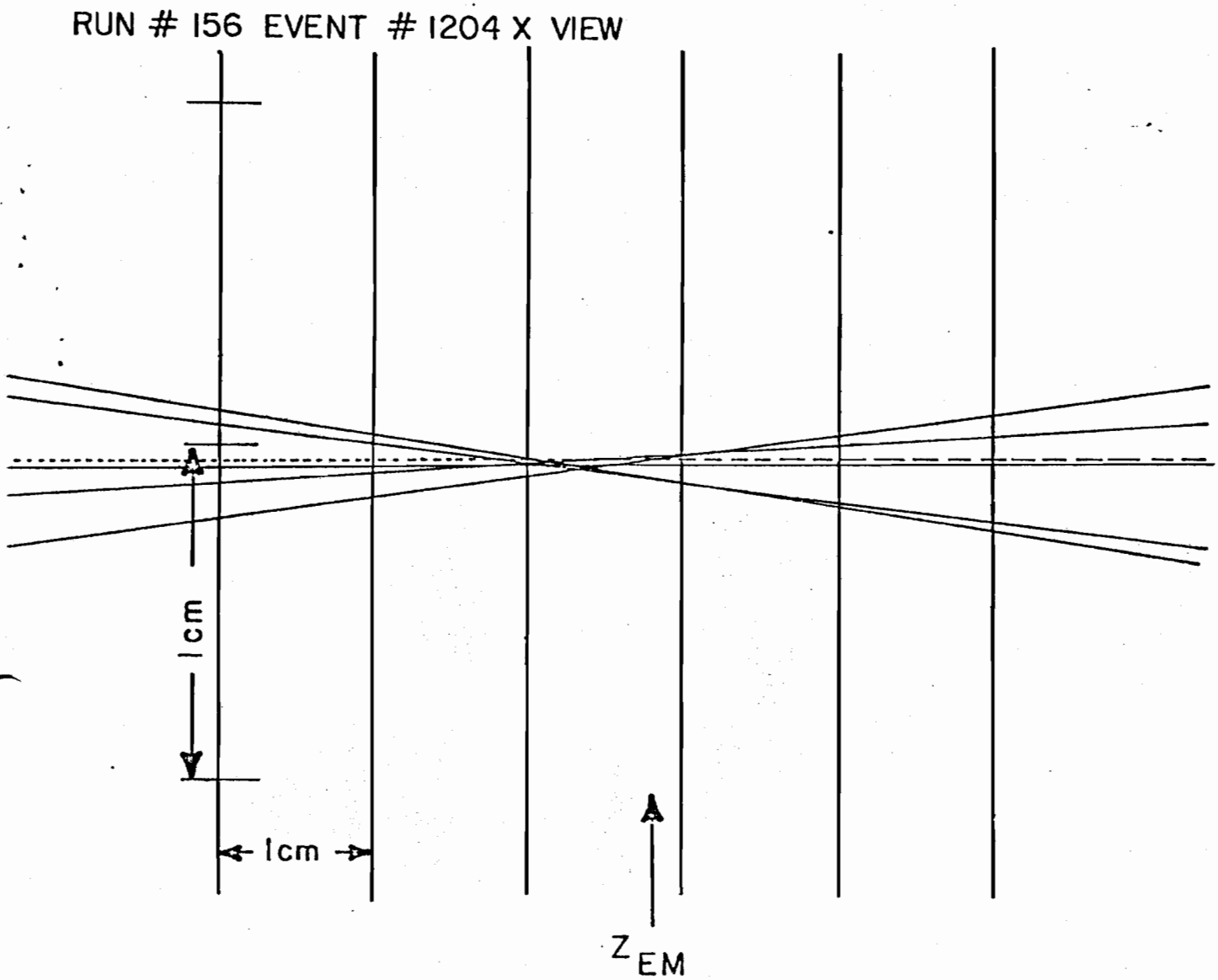

DC-PC VERTEX RECONSTRUCTION

Figure 3a

cc9c273

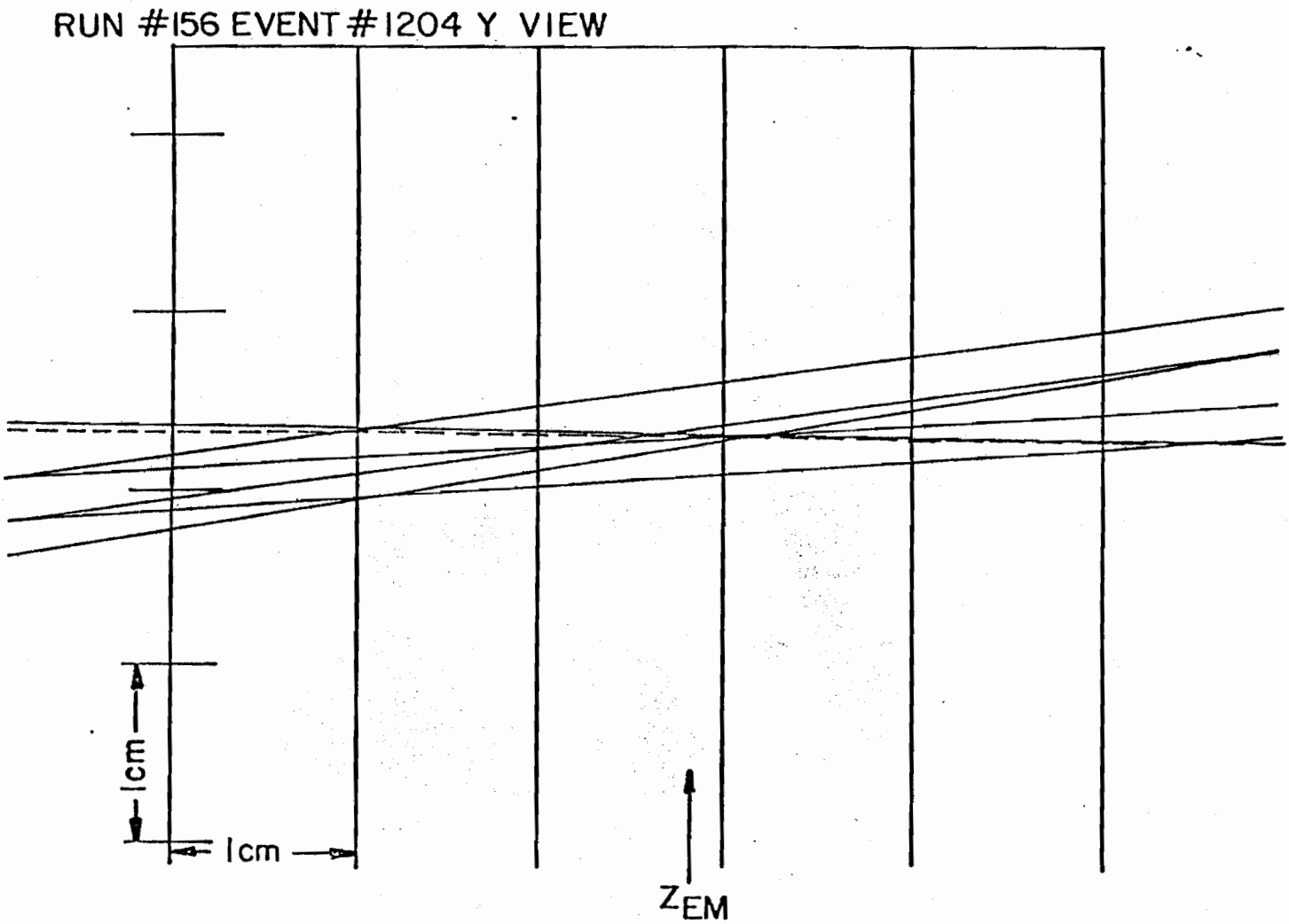

DC-PC VERTEX RECONSTRUCTION

Figure 3b

cu9020

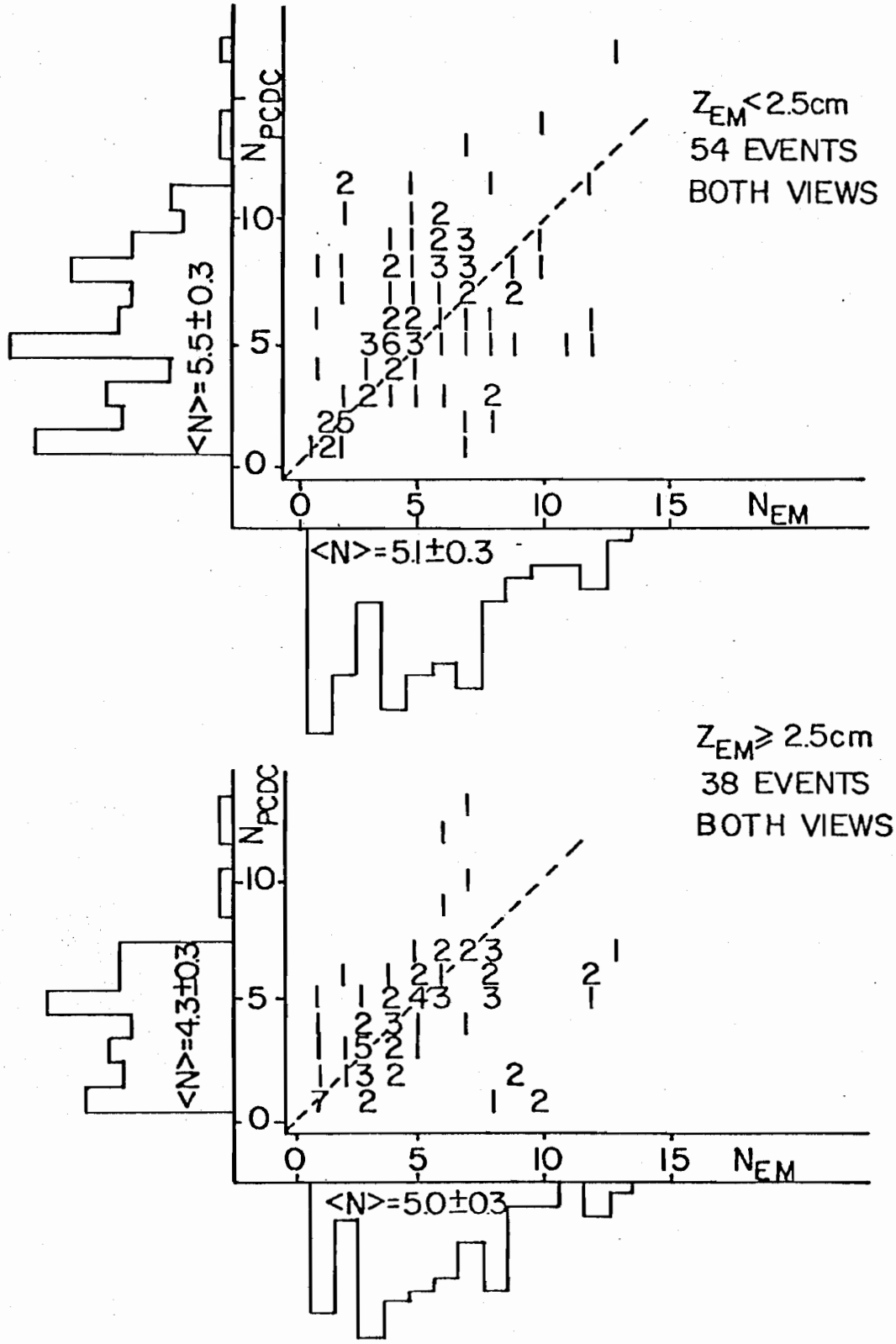

Figure 4

C2902 77

PCDC- ONE PROJECTION MATCHES
VS EMULSION TRACKS

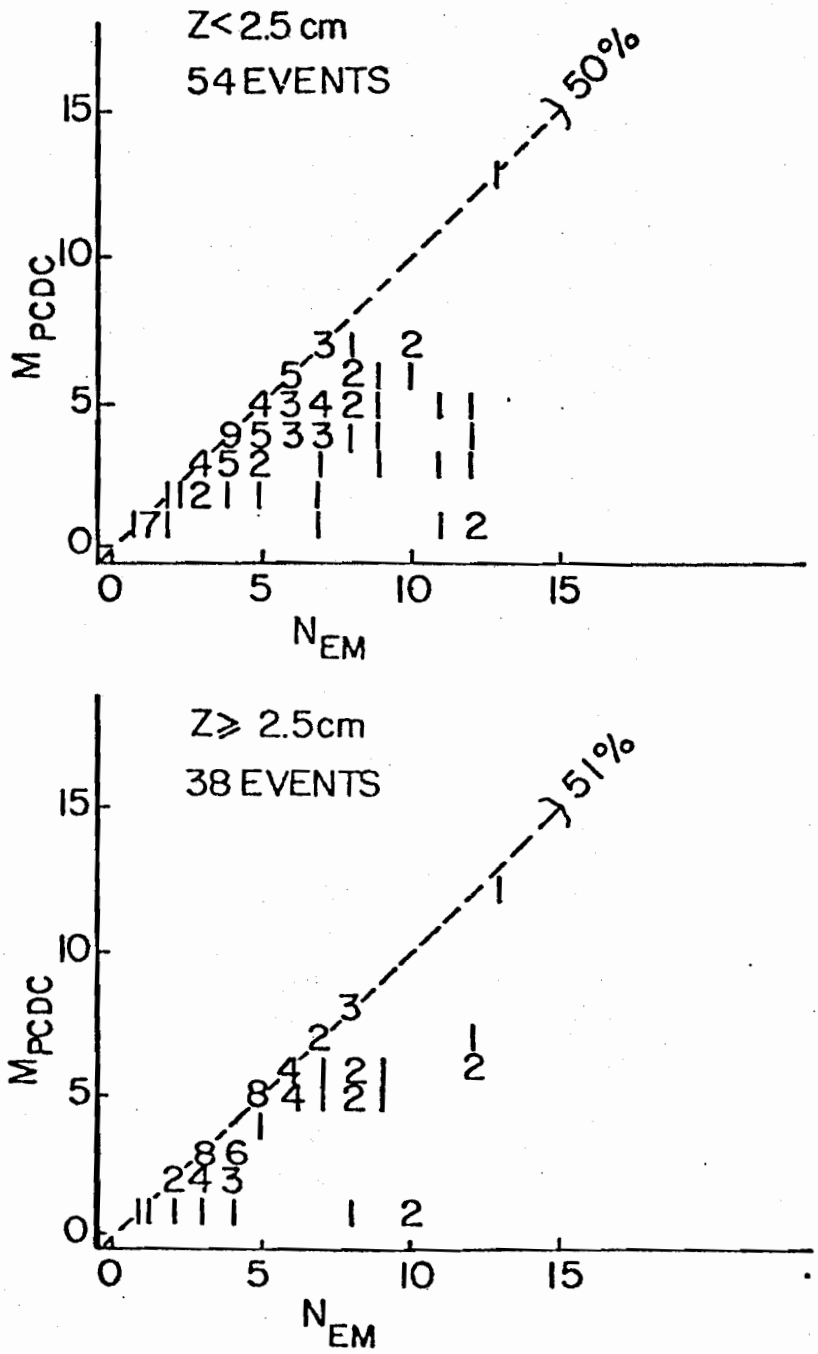

Figure 5

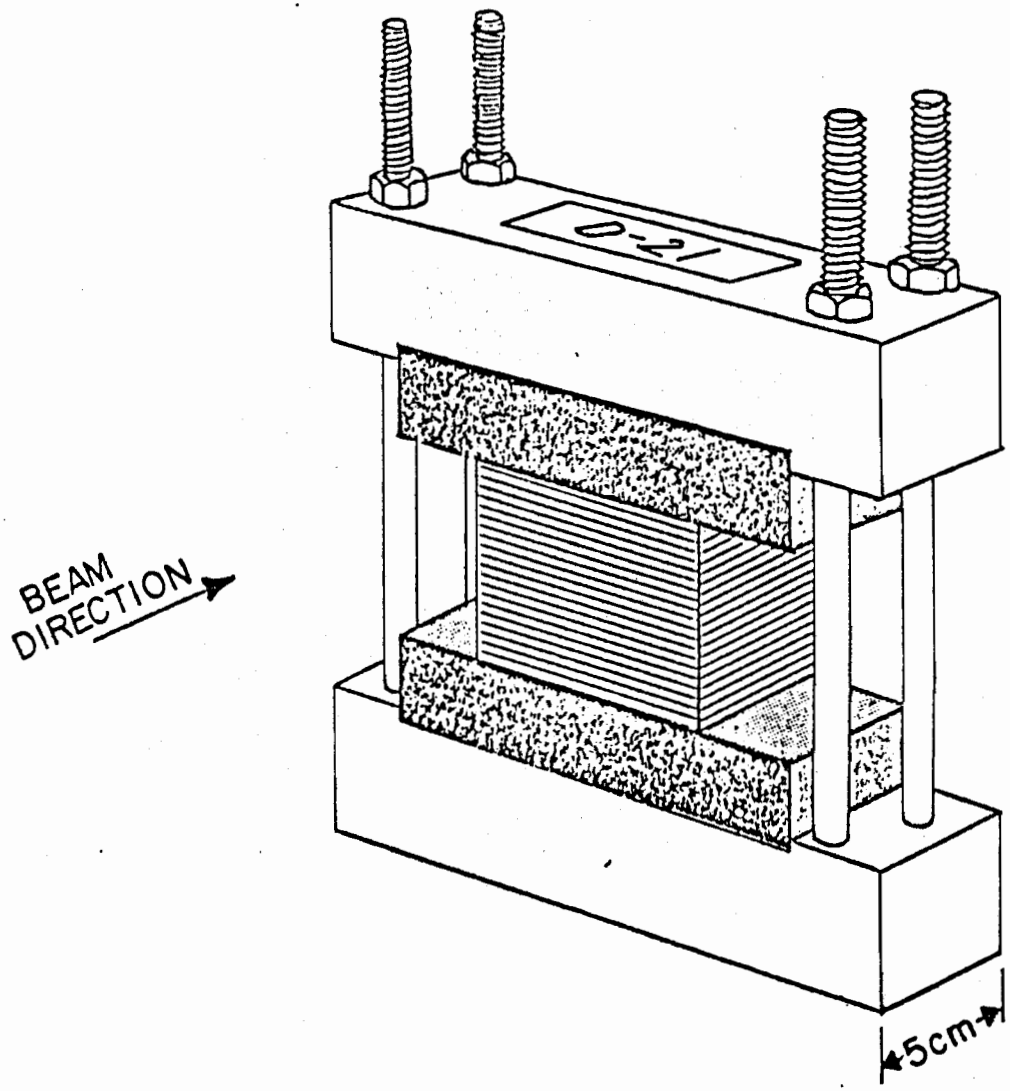

Figure 6

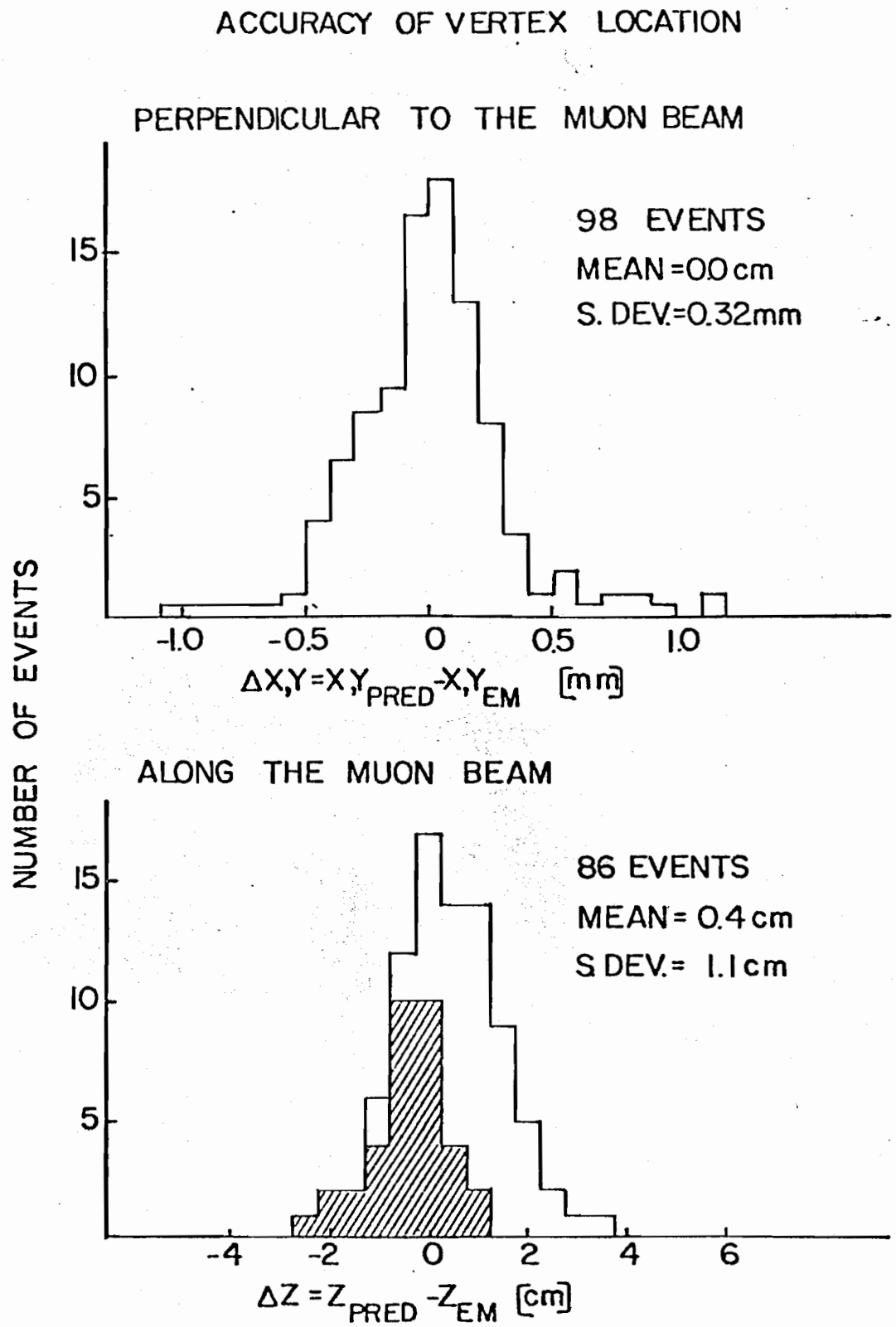

Figure 7

C290279

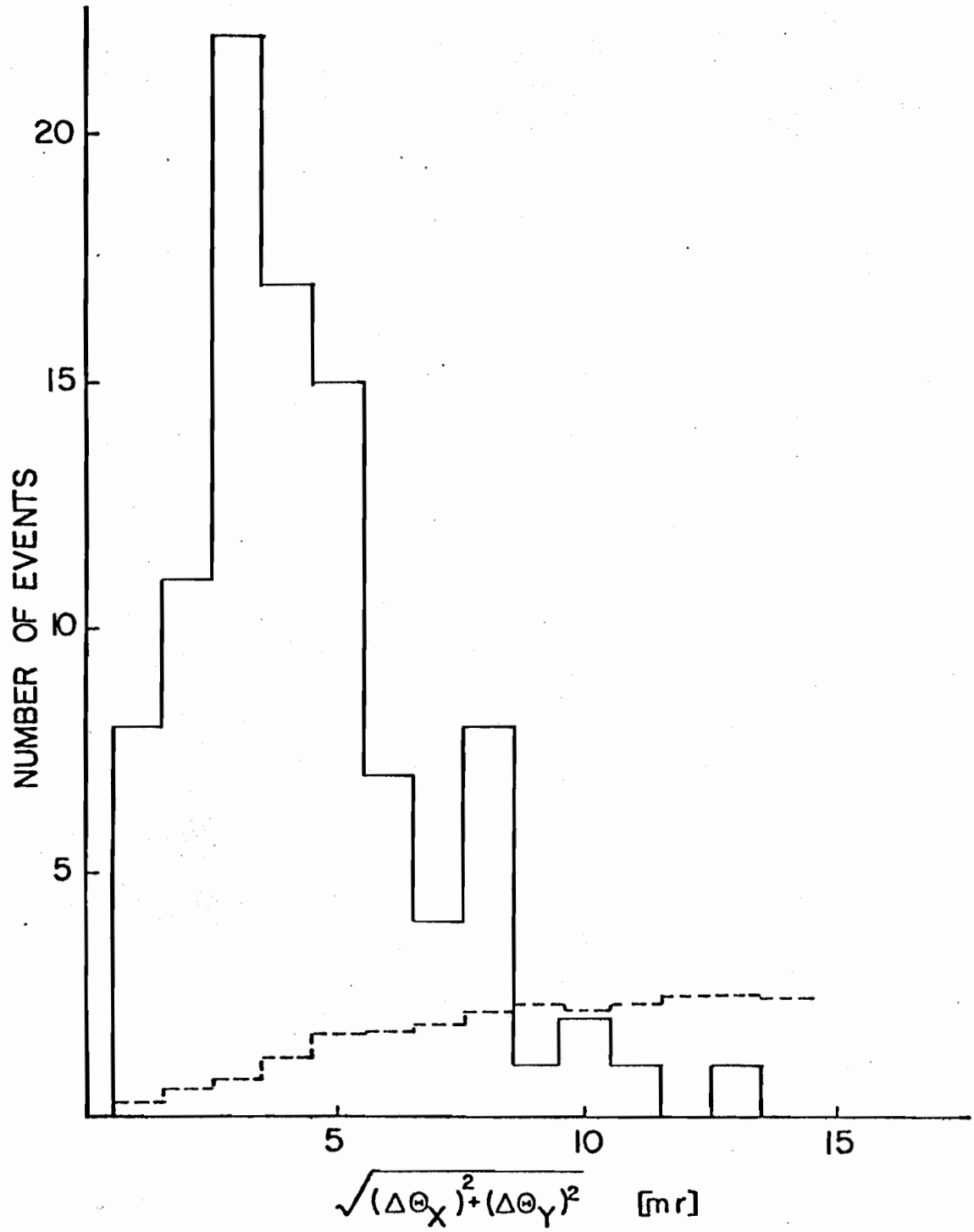

Figure 8

0290279

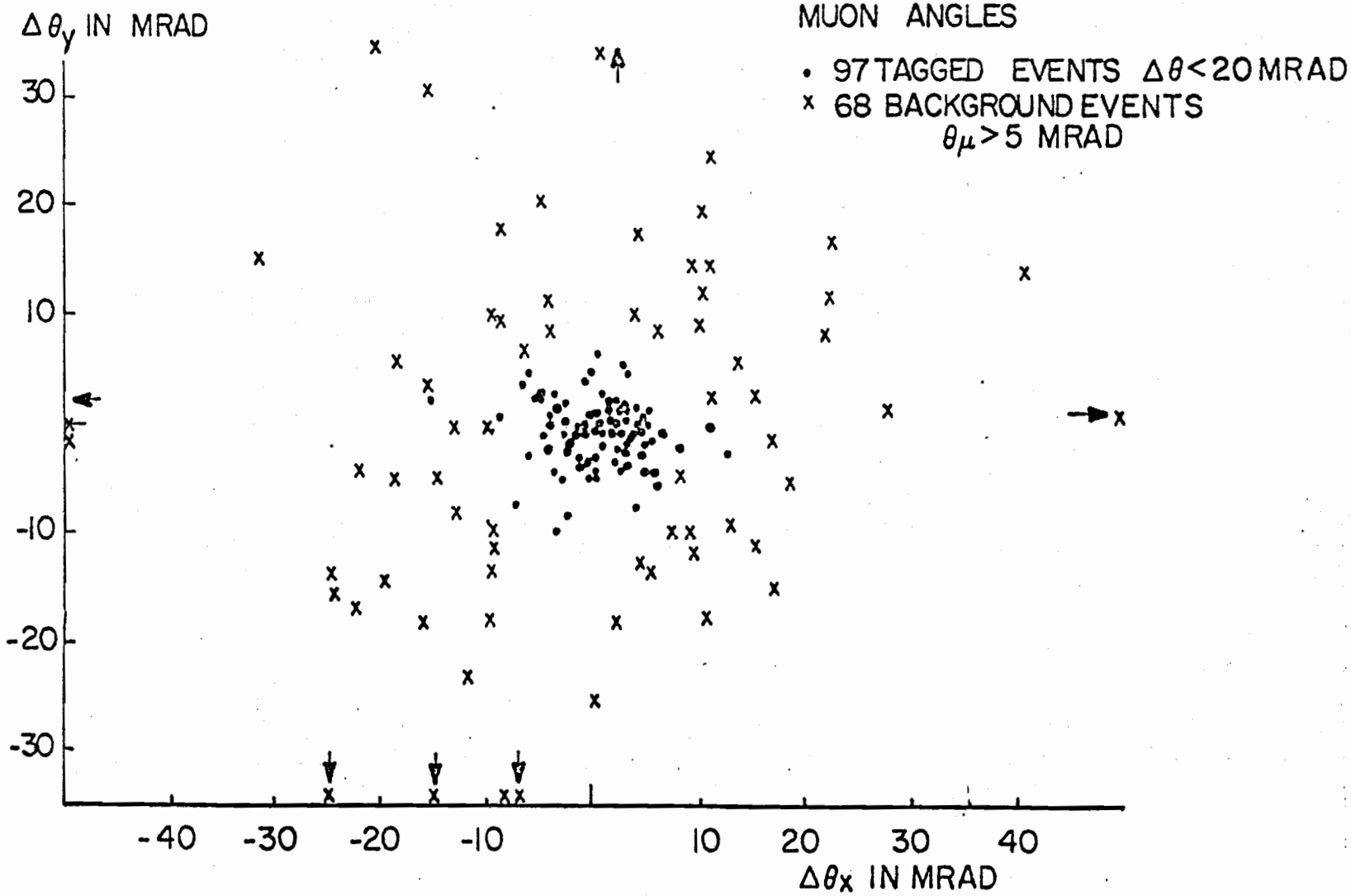
SCATTER PLOT OF THE DIFFERENCE BETWEEN PREDICTED AND OBSERVED MUON ANGLES
• 97 TAGGED EVENTS Δθ<20 MRAD
x 68 BACKGROUND EVENTS θμ>5 MRAD
Δθy IN MRAD
30
20
10
-10
-20
-30
-40
-30
-20
-10
10
20
30
40
Δθx IN MRAD

Fig[illegible] 9